Technological Applied Sciences Status : Review
ISSN: 1308 7223 Received: 11.07.2025
Article ID: 2A0212 Accepted: 15.01.2026

İhsan Kırık
Bingöl University, alihsankirik@gmail.com, Bingöl-Türkiye

DOI	http://dx.doi.org/10.12739/NWSA.2026.21.1.2A0212
ORCID ID	0000-0002-8361-319X
Corresponding Author	İhsan Kırık

MECHANICAL PROPERTIES AND FATIGUE BEHAVIOR OF ALUMINUM ALLOYS JOINED BY CO_2 LASER WELDING: A REVIEW

ABSTRACT

Due to its high energy density and flexibility, laser welding of aluminium alloys has gained significant prominence in high-performance sectors such as aerospace, automotive, and the chemical industry. This study provides a comprehensive review of current laser welding technologies for aluminum alloys, with a focus on metallurgical challenges and the mechanical properties of the joints. Unlike conventional arc welding, precise control over various process parameters is required for laser welding of aluminium to mitigate common defects. A critical analysis of the literature suggests that, regardless of its spatial location within the weld, porosity remains the primary factor that degrades fatigue strength. This research notably distinguishes between technical porosity, which can be eliminated through parameter optimisation, and metallurgical porosity (e.g., hydrogen- or metal vapour-induced), which tends to localise near the weld surface. Although CO_2 and modern fibre laser technologies have improved the reliability of these joints, this study reveals an ongoing gap in the literature concerning the fracture toughness, detailed microstructural characterisation, and long-term fatigue behaviour of specific laser-welded aluminium alloys. This review serves as a technical foundation for future research aimed at optimising joint integrity in structural applications.

Keywords: Al and Alloys, Laser Welding, CO_2 Laser Welding, Mechanical Properties, Fatigue Behavior

1. INTRODUCTION

In the aerospace industry, a focus on weight reduction and damage tolerance is crucial for ensuring safer flights and increasing load-carrying capacity [1 and 2]. Therefore, structural materials that are resistant to fatigue cracking are preferred. Furthermore, using welded integrated structures instead of riveted connections can reduce structural weight even further [3 and 4]. Due to their lower density, greater specific strength and elastic modulus, superior resistance to fatigue fracture propagation and corrosion, aluminium alloys are favoured for use in aircraft [5, 6, 7, 8, 9, 10, 11, and 12].

Laser welding (LW) is a thermal joining method that uses a laser to join metals or plastics. It is a deep-penetrating keyhole welding technique, which is generally used in engineering applications despite the high cost of the initial equipment required. In laser welding, the energy transferred to the welding area differs from that in other methods; the light beam emitted from the environment is transferred to the focal centre by reflection. This ensures a narrow welding area, providing the advantage of localised melting and vaporisation of the material in terms of area density. During plasma condensation, the shielding gas and vaporised material are transferred to the workpiece

How to Cite:
Kırık, İ., (2026). Mechanical properties and fatigue behavior of aluminum alloys joined by CO_2 laser welding: a review. Techonological Applied Sciences, 21(1):1-18, DOI: 10.12739/NWSA.2026.21.1.2A0212.

with laser energy. The molten metal rises to the surface of the workpiece due to the pressure of the heated steam while simultaneously preventing expansion caused by attractive forces, viscosity, and surface tension. Using this method, the metal melts depending on the direction in which the laser beam moves, while the remaining molten portion solidifies. After solidification, a narrow weld seam with a homogeneous structure is formed. In a weld seam created with low heat input, the heat-affected zone (HAZ) in the workpiece remains within very narrow limits. This method is generally used to weld thick sheets by creating a weld pit [13 and 14]. Figure 1 shows a schematic representation of laser beam welding.

In laser welding applications, two types of laser systems are typically employed: CO_2 lasers and Nd:YAG (neodymium-doped yttrium aluminium garnet) solid-state lasers. CO_2 lasers are used for macroscale welding processes (for thicknesses of 1–15 mm), while Nd:YAG lasers are generally preferred for microscale welding processes (for thicknesses of 0.2–4 mm). Nd:YAG lasers enable high-quality welding at relatively high speeds [15]. The welding method varies depending on the energy density of the laser beam. Figure 2 shows two different methods: conduction welding for thin materials and penetration (keyhole) welding for thicker materials [16]. Porosity is infamous for weakening joints and reducing mechanical quality. As magnesium evaporates easily during welding, high-Mg-content Al–Mg alloys are prone to forming pores [51, 52, 53, and 54]. Macroscale porosity in joints can be significantly reduced by modifying the welding conditions. The efficacy of this technique when laser-arc welding Al–Mg alloys with other kinds of Al alloys is still unknown. Furthermore, micropores have been found to negatively affect the fatigue strength of welded joints; however, their effect on joints made from different aluminium alloys has not been thoroughly studied.

The literature provides extensive data on the interaction between different types of lasers and aluminium alloys. To facilitate a clearer understanding of these complex relationships, the experimental studies, process parameters, and key findings have been categorised according to the laser technology and welding method employed (see Tables 1, 2, and 3).

Table 1. CO_2 and Nd: YAG Laser Applications on Aluminum Alloys

Materials/thickness	Main types of lasers	Process parameters	Remark	Ref.
A3003, A7N01, A5052 and A5182 (5-7mm)	5Kw CO_2 laser,	Power, kW, q (3-5) Speed, mm/sec (17-100) Defocus distance (2mm)	The magnesium and hydrogen contents of Al alloys have a significant impact on porosity formation.	[23]
AA 7020 (3mm)	A Lumonics 200 MW pulsed Nd: YAG laser, Helium gas	power of 1.9kW, frequency of 100 Hz, and travel speed of 0.4 m/min	There was a small heat-affected zone where the base metal gave way to the fused zone. Strong zinc depletion was noted, as hot fractures were not seen in the weld zone; this did not affect the hot tearing susceptibility.	[32]
A5182P-O aluminum 1 and 7mm thickness	$C0_2$ laser of 5.5kW maximum power	Power 5kW crosshead speed 0.033-0.083 (mm/s)	Using the specimens with artificially drilled holes, it was verified that the strength significantly dropped as the hole or porosity size increased.	[35]
A356 and AA5083 aluminum alloys	Nd: YAG laser welding	Power 4kW	It was determined that dual-beam welding and	[39]

(4mm)		welding speeds 2-5 m/s helium shielding A 20l/min	surface preparation are sufficient techniques for lowering the potential for porosity formation in laser assemblies.	
A5754-O Al-Mg	Rofin-Sinar CW025, 2.5kW Nd: YAG laser system Argon shielding gas	Power 1.5kW gas flow rate: 15-20L/min	Compared to P, F has a far greater impact on the mechanical characteristics, hot fracture susceptibility, microstructure, and weld bead geometry. Nevertheless, P has a greater impact on the welding speed change than F.	[42]
AA5052, AA5083, and AA6061 Aluminum Alloys (2mm)	laser welded 5kW CO_2 laser machine	laser power 3-5kW welding speed 4m/min	Tensile testing and hardness measurements of AA6061 alloy welds revealed a notable softening of the fusion zone because of the dissolution of the strengthening precipitates, which was restored by aging treatment following welding. Compared to the AA6061 alloy, the softening of the fusion zone caused by the loss of its work-hardened condition was significantly less for alloys AA5052 and AA5083.	[43]
Wrought AM60 magnesium alloy (1.6mm)	3.0kW continuous wave CO_2 laser	Laser power 0.6-1kW Welding speed 1.5-3.5m/min	Tensile testing results indicate that the joints' maximum ultimate tensile strength (UTS) can reach up to 94% of the base metals.	[48]
A5083 10 mm thick aluminum	5 kW laser (IPG YLS-5000) Nd: YAG laser beam	Pressure 10^3-10^{-3}Pa Laser power 2000W Welding Speed 0.8m min 1^{-1}	The critical ambient pressure required to increase the penetration depth and tensile strength of the joints during the subatmospheric laser welding process was 10^{-1} Pa.	[50]

In addition to the more traditional CO_2 and Nd: YAG systems, recent technological advances have given rise to high-brightness fibre and disk lasers. Table 2 summarises the specific parameters and outcomes associated with these modern laser sources.

Table 2. Fiber and disk laser applications on aluminum alloy

Materials/thickness	Main types of lasers	Process parameters	Remark	Ref.
AA 5083-H32 (6mm)	Yb: YAG diode-pumped disk laser shielding gases (Argon (Ar), Helium (He), Nitrogen (N), and a mixed gas (Ar-	Laser power (kW)2.5-3.5 Welding speed (10-60mm/s)	Grain development, Al6 (Mn, Fe) production, and dendritic structure have all been seen in the heat-affected zone (HAZ). The formation of the porosity was explained by the shielding gas being trapped because of the keyhole collapsing.	[25]

	O2 (100 ppm)- NO (200 ppm)			
AA5052 (1 mm)	2kW ytterbium fiber laser of 1064 nm	Power kW 1.2 Scan speed mm/s 610 Heat input J/mm 1.97	Because of its smaller average grain size, the MBW had the maximum tensile strength (208.2 MPa, or approximately 91% of the basic material's tensile strength). It was discovered that the laser welding-induced re-crystallization process greatly enlarged the original material's grain size.	[33]
CR340 steel produced by cold rolling and 6061-T6 Al alloy (1.2-1.5mm thickness)	The IPG YLR-6000 fiber laser	Laser power, kW 2 Welding-brazing speed, 5 mm/s Wire filling speed, 20 mm/s	Numerical simulation findings also demonstrated that an increase in CO_2 levels resulted in greater peak temperatures.	[36]
2219 aluminum alloy T (2.5-3.5mm)	TruDisk12003 disc laser, T-joints DLBSW process	Laser power 4.3-5 kW	Furthermore, by enhancing the welding settings, technical porosity—which is primarily located in the middle or bottom of the weld seam—can be removed. Metallurgical porosity, such as hydrogen porosity and metal vapor porosity created by the burning of metal elements, is primarily found near the top and edge of the weld seam.	[37]
DP590 steel and 6061 Al (1.2 and 1.5 mm)	PG YLS-4000 laser weld, KR60HA robot	Power of 4kw. multi-modes. length of 250mm. focus of 0.42mm.	As the crystal structure developed, internal stress caused the crack to widen and take on a radial pattern during the cooling phase.	[38]
(T6) 6061 aluminum alloy and 4043 filler wire (1.8mm)	YAG laser beam and CO_2 laser beam	CO_2, 7.8 kW, Speed, 4 m/ min	The welded T-joint displayed a nice weld appearance with no macro flaws at the optimal parameters; the tensile strength was approximately 254 MPa with the fracture at the heat-affected zone on the stringer side, and the micro hardness of the welds varied from 75 to 85 HV 0.3.	[41]
AA6061 aluminum alloy 4T (1mm)	TRUMPF TruLaser Cell 3000 coupled with a Yb: YAG 3.3 kW source. Yb: YAG laser beam	Power 1.5-2.5 kW Welding travel speed 2-4 min/m Energy density 637-171 $J.mm^2$	The hardness in the FZ was lower than that of the base material (BM), and it was the same in the HAZ. The welding parameters determined the FZ hardness. Strain measurements using digital image correlation (DIC) revealed greater deformation close to the FZ, but the FZ deformed more uniformly once geometrical flaws were fixed.	[45]
AA 6061 Aluminum (2mm) ER4047 filler wire	Laser beam welding	Power 1.9-2.9 kW, welding	Nanoindentation studies revealed a little softening in the heat-	[46]

		speed 2m/min to 3m/min	affected zone caused by recrystallization. Every specimen failed in the weld metal, and the fracture surfaces displayed ductile fracture characteristics.	
Al–Mg–Si–Cu alloy 6013 sheet (1.6mm)	Nd: YAG laser 3kW	Power 3 kW welding speed was 3–4 m/min	Welds showed non-corroded zones next to the fusion boundaries in the as-welded T6 condition. Alternate immersion tests in a 3.5% NaCl solution did not reveal these corrosion-free zones. When submerged in an aqueous chloride–bicarbonate solution, welded 6013-T4 joints were vulnerable to stress corrosion cracking in the heat-affected zone.	[47]
Wrought aluminum alloy	Laser beam welding	-	Consequently, the basic issues surrounding the use of laser welding technology on aluminum alloys are gradually being reduced.	[49]
AA2024-T4 thickness 2 mm	Nd: YAG laser welding power 400 W	Pulse peak power, 1.2 kW Laser travel speed, mm s^{-1}	Shrinkage brittleness theory may be the basis for the mechanism of cracking in the columnar zone, whereas strain theory may be the basis in the equiaxed zone.	[52]

To overcome limitations such as the bridgeability of gaps and porosity in thick sections, hybrid systems combining laser power with traditional arc methods have gained prominence. Table 3 provides details of the process dynamics and metallurgical observations of hybrid laser-MIG welding applications.

Table 3. Hybrid Laser-MIG and special laser processes

Materials/thickness	Main types of lasers	Process parameters	Remark	Ref.
AW5083 aluminum (2mm) 5087 filler wire	Butt laser weld, Ar + 30 vol. % He shielding gas	Laser Power (kW)(1.9) Welding speed (20mm/s)	Al2O3 particles led to a brittle fracture of the unshielded weld junction.	[24]
AA 6082-T6 (6mm)filler wire ER5356	laser-MIG hybrid butt-welded	Laser power P/kW (2.4-3.9) Arc current I/A (140) Welding speed V/ m/min (0.72-2.4)	When the porosity rate grew from 0% to 8.9%, the fatigue strength decreased from 113 MPa to 56 MPa, although the porosity location had no impact. When there was no porosity in the joint, the fracture started in the weld surface; when there was porosity, it started close to the porosity.	[26]
A7N01-T5 Welding wire ER5356 (8mm)	PG YLS-4000 fiber laser, a KEMPI KempArc-450 pulsed MIG welding machine1,070-µm wavelength, 200-µm core diameter, and	Welding speed (m/min) 0.54 Laser power (kW) 3.2 MIG current intensity (A)207	Because of its as-cast structure with equiaxed grains and coarse particles, the FZ has the lowest microhardness and tensile strength (173 MPa). The tiny, uniform strengthening-phase particles that cause the	[27]

	310-mm focusing lens.		dislocations to migrate in a sheared manner are responsible for the BM's highest microhardness and tensile strength (370 MPa).	
AA5083 and AA7N01	hybrid laser-MIG welding IPG YLS-4000 fiber laser	Laser power 1.3kW Arc current 130A Welding speed 0.64-1m/min	SEM findings show that pores and inclusions are the primary causes of fatigue strength degradation. Furthermore, the yield strength, strain rate hardening, and work hardening behavior of the fusion zone are successfully simulated using a strength model.	[28]
5A06 Aluminum Alloy ER5356 filler wire	Laser-MIG hybrid welding	Laser power (kW)3.5 Welding velocity (m/min)1.2-1.5 Welding current (A)135-170	The pore wall has a higher element content of Mg and O than the dimple. The presence of coarse pores in the laser-MIG hybrid-dominated region impedes the formation of equiaxed dendritic grains during the solidification process. Insufficient research has been done on the effects of different Al alloys on joints.	[29]
AA 5083 ER5183 filler wire	The laser-GMAW processes	Laser power (Kw) 3-4.9 Welding speed(m/min) 2 Arc current(A)100	Because there is less porosity creation, a minor loss of magnesium, more uniformly distributed second-phase particles, and the formation of dislocations with higher density in the joints, the strength of the joint is better in the LAHW process, even if the grain size is larger.	[30]
AA5083 and AA6082(4mm) ER5356 ER4043 filler wire	Laser-MIG welding method	Arc current (A) 152-173 Arc voltage (V) 21.2-23.6 Laser power (kW) 1.2Welding speed (m/min)2.2	Molecular dynamic simulation reveals that the high density of pores in the FZ of ER4 joints is responsible for the loss of mechanical characteristics because these pores induce significant stress concentration under external uniaxial loading.	[31]
GH909 Al alloy 10 mm	Laser-MIG hybrid welding	Laser power 4000W Welding speed0.54-0.9 m/min Welding current 110-144A	The joints' average tensile strength was 632.90 MPa, or almost 76.84% of the base metal. According to the fracture analysis, the joint's fracture mode was ductile fracture, and the emergence of porosities created in the welding process was the primary cause of joint failure.	[34]
AA 6063-T6 Al S30403 stainless steel (2mm) ER4043 filler wire	laser-MIG hybrid welding-brazing process.	Laser power 2kW, Welding speed 20mm/min Feeding rate 4.5m/min	The strength and ductility of the joints rose by 18.4% and 191%, respectively, as compared to joints welded in a pure argon atmosphere.	[40]

		Welding current 92-95A		
5A06 aluminum (15mm) ER5356 filler wire	Narrow-gap rotating laser welding, rotating laser welding	Laser power 4 kW, Defocus distance 5mm, Diameter of rotation 0-2mm, Rotation frequency 0-50, Welding speed 0.3m/min	The recrystallization temperature of 5A06 aluminum is exceeded by the maximum temperature of HAZ, which is greater than 280 °C. Additionally, there appears to be a bimodal distribution of residual stress in the thickness direction.	[44]

As can be seen from these tables, the management of porosity and the preservation of mechanical properties in the fusion zone (FZ) remain the primary focus of contemporary research, regardless of the laser type.

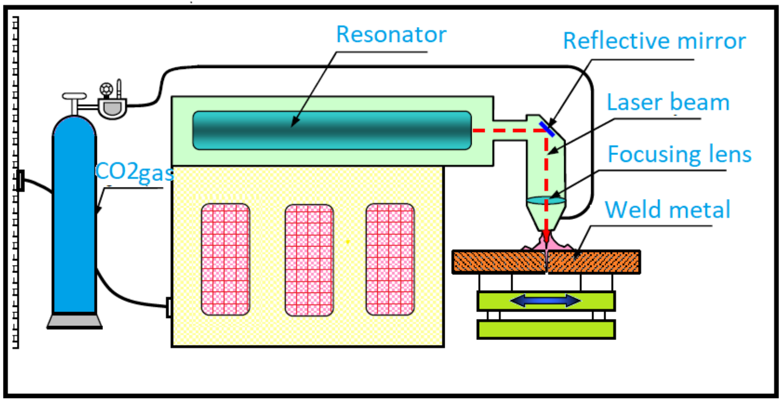

Figure 1. Laser welding source equipment [17].

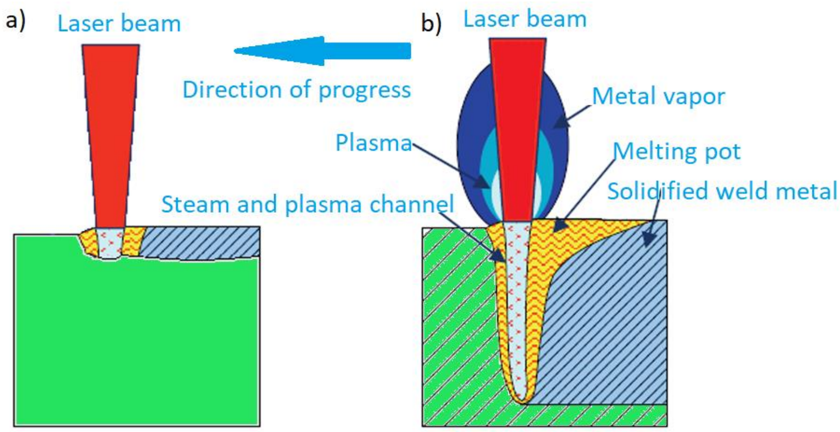

Figure 2. a) Laser transmission and b) penetration source [18]

2. RESEARCH SIGNIFICANCE

This study is important because it addresses the aerospace industry's critical need for lightweight, damage-tolerant, and fatigue-resistant structural materials, which can enhance flight safety and load-carrying capacity. Using aluminium alloys in combination with laser welding technology offers significant advantages over traditional riveted structures, as it reduces structural weight while maintaining high mechanical performance. Laser welding, particularly with Nd: YAG systems, enables the production of narrow, high-quality weld seams with low heat input and minimal heat-affected zones. This is essential for preserving the fatigue and corrosion resistance of aluminium alloys. Therefore, understanding and optimising laser welding processes for aerospace-grade aluminium alloys contributes directly to the development of safer, lighter, and more efficient aircraft structures.

Highlights

- Laser welding of aluminium alloys enables significant weight reduction in aerospace structures by replacing traditional riveted joints with integrated welded designs.
- The low heat input and narrow heat-affected zone of laser welding help to preserve the fatigue resistance, corrosion performance and structural integrity of aerospace materials.
- Using Nd: YAG laser systems enables the high-quality, high-speed welding of thin aluminium components, supporting safer and more efficient aircraft manufacturing.

3. EVALUATION AND METALLURGICAL CHARACTERISTICS OF LASER WELDING

3.1. Advantages of the Laser Welding Method

- Compared to other fusion welding methods, laser welding enables faster welding with deeper penetration. As the heat input is concentrated in a small area, deformation and warping may be minimal or non-existent [19].
- Laser welding can also be used alongside other welding methods.
- Thick samples can be welded using laser-arc hybrid welding, and large weld gaps can be joined using multiple passes [20].
- The laser beam can be focused on a small area. This is considerably smaller than in classical fusion welding. Therefore, it is frequently used for joining very thin parts and for cutting operations [21].
- It is suitable for automated systems, easily adapting to existing production systems, and is aesthetically pleasing.
- It produces narrow, reliable weld seams with a high depth/width ratio, eliminating the need for post-welding processing such as grinding.
- It can weld difficult-to-weld materials and dissimilar materials. The results are very good.
- It allows for easy welding of areas that are difficult or impossible to reach with traditional methods.

Laser welding is more advantageous than other methods due to its high heat density and small beam focusing diameter. Consequently, the microstructure change in the weld area is quite narrow.

Deep, narrow welds are created.

- It is more resistant to wear than traditional methods due to its finer, harder microstructure.
- Hard grain growth and metallurgical damage caused by the large heat-affected zone (HAZ) are minimised by this welding method.
- Part design possibilities are favourable.
- Even very small and thin materials can be welded.
- It allows welding in narrow and specific areas.

3.2. Disadvantages of Laser Welding:

- Due to the narrowness of the laser beam, the surfaces to be welded must be flat.
- Due to the depth/width ratio and height of the weld area, it is difficult to insert the filler metal.

- The high reflectivity of the metals to be welded makes laser welding difficult.
- Using pulsed laser welding on hard materials creates microscopic weld cross-sections, which makes the weld brittle.
- The high initial investment cost of laser welding is a disadvantage.

3.3. Microstructure Analysis of Welded Joints in Different Aluminum Alloy Series

The microstructural evolution of aluminium alloy welded joints depends heavily on the composition of the alloy, the strengthening mechanism, and the thermal cycle imposed during welding. Fusion welding generally produces three distinct regions — the base metal (BM), the heat-affected zone (HAZ) and the fusion zone (FZ) — which exhibit different grain structures and precipitate distributions, as shown in Table 4.

- **Al–Cu Alloys:** In the Al–Cu series of aluminium alloys, the weld metal usually has a refined equiaxed grain structure because of rapid solidification. However, significant dissolution of the strengthening θ′ (Al_2Cu) precipitates occurs in the heat-affected zone (HAZ). This leads to localised softening and a reduction in hardness and tensile strength in the HAZ. Additionally, partial grain coarsening frequently occurs near the fusion boundary, further contributing to the degradation of mechanical properties in this region [55].
  Al-Cu series aluminium alloys are another class of aluminium alloys that are widely used in the automotive sector. Copper is the primary alloying ingredient in these alloys, followed by magnesium. Casting is used to create aluminium alloys in the Al-Cu range. Despite having high strength values, the Al-Cu series aluminium alloys have limited corrosion resistance compared to other aluminium alloys. Consequently, they cannot be used in high-temperature applications [56]. Al-Cu (7–8% Cu) alloys are among the alloy classes with the best high-temperature characteristics of cast aluminium alloys. The chemical composition of this alloy can be enhanced by adding copper, nickel, magnesium, and occasionally iron to increase its resistance to wear at high temperatures. Both casting and powder metallurgy (Mahle) can be used to produce aluminium alloys. This improves mechanical properties and corrosion resistance and enables the creation of a purer microstructure. However, a purer microstructure can be produced using mechanical alloying or quick cooling. These techniques allow microcrystalline phases to be created and lattice imperfections to be reduced [56, 57, and 58].
  Al-Li-X alloys are favoured over the Al-Cu and Al-Zn-Mg series of aluminium alloys due to their low density, high modulus of elasticity, superior fatigue strength, and favourable toughness characteristics [58]. Like Al-Cu, Al-Mg-Si, and Al-Zn-Mg alloys, aluminium lithium alloys can also be subjected to precipitation hardening heat treatment [59]. However, the phases created by precipitation hardening break down at high temperatures, resulting in a loss of strength. Consequently, aluminium-lithium alloys cannot demonstrate adequate strength at high temperatures despite their favourable strength-to-density ratio [59].
- **Al–Mg Alloys:** Due to the solid solution strengthening mechanism of magnesium, the weld metal of Al-Mg alloys has uniform, fine grains with minimal precipitation effects. Grain development in the heat-affected zone (HAZ) is often moderate, although there is

no significant precipitate dissolution. However, β (Al_3Mg_2) phases may form or grow along grain boundaries in high-magnesium alloys, which can reduce corrosion resistance and ductility slightly [60].

- **Al-Mg-Si Alloys:** Microstructural analysis of Al-Mg-Si series alloys reveals substantial changes in the heat-affected zone (HAZ), where Mg_2Si strengthening precipitates dissolve during thermal cycles of welding. The weld metal consists of fine dendritic or equiaxed grains, depending on the cooling rate and the composition of the filler. The dissolution and subsequent non-uniform reprecipitation of Mg_2Si result in a soft zone forming in the HAZ. This zone commonly governs the location of tensile failure in welded joints [40 and 47]. The characteristic properties of different types of aluminium alloy are compared in Table 5.
- **Al-Zn-Mg-Cu Alloys:** Welded joints of Al-Zn-Mg series alloys have a refined grain structure in the fusion zone, whereas the HAZ undergoes extensive precipitate dissolution and over-ageing. The η′ and η ($MgZn_2$) strengthening phases are particularly sensitive to welding heat input, resulting in a notable reduction in hardness in the HAZ. Grain coarsening near the fusion line intensifies this heterogeneity further, often causing the HAZ to become the weakest region of the joint [67].
- Many techniques have been developed for joining materials with different properties. Tungsten inert gas welding is suitable for Al-Mg-Si alloys, but often causes cracking and porosity in Al-Zn-Mg alloys. High heat input widens the HAZ and softens the joint [61]. Although friction stir welding eliminates the melting condition, it lacks flexibility for complex shapes [62]. Laser welding, however, has high energy density, a narrow HAZ and good flexibility, and is therefore widely used for different aluminium alloys [63, 64, 65, 66, and 67].

Table 4. Comparison of aluminum alloy series

Property	Al-Mg	Al-Cu	Al-Mg-Si	Al-Zn-Mg
Main alloying element(s)	Mg	Cu	Mg + Si	Zn + Mg
Strengthening mechanism	Solid solution	Precipitation	Precipitation	Precipitation
Heat-treatable	No	Yes	Yes	Yes
Strength level	Medium-high	High	Medium	Very high
Ductility	High	Medium	High	Low-medium
Corrosion resistance	Excellent	Poor-moderate	Good	Moderate
Weldability	Excellent	Poor	Good	Moderate poor
Suitability for marine use	Excellent	Not suitable	Limited	Not suitable
Typical applications	Marine structures, tanks, automotive	Aerospace structures	Extrusions, structural parts	Aerospace, defense
Common alloys	5052, 5083, 5754	2024	6061, 6082	7075

Table 5. Welding metallurgy characteristics of aluminum alloy series

Alloy Series	Main Strengthening Phase	HAZ Microstructural Change	Weld Metal Grain Structure	Typical Weld Defect / Weakness	Mechanical Consequence
Al-Cu	Al_2Cu (θ)	Extensive precipitate dissolution, grain growth	Columnar / dendritic	Hot cracking, severe softening	Large strength loss in HAZ
Al-Mg	Solid solution (Mg)	Moderate grain growth, possible β(Al_3Mg_2) at GBs	Fine equiaxed	Intergranular corrosion (high Mg)	Slight ductility reduction

Al-Mg-Si	Mg_2Si	Precipitate dissolution + partial reprecipitation	Fine dendritic or equiaxed	Soft zone in HAZ	Tensile failure in HAZ
Al-Zn-Mg	$MgZn_2$ (η)	Dissolution + overaging	Columnar / equiaxed	Hot cracking, SCC	Severe softening + cracking risk

3.4. Mechanical Properties

Tensile testing of CO_2 laser-welded aluminium alloys typically indicates that joint tensile strengths are approximately 80–95% of those of the base metal. This level of retention depends strongly on the alloy series and the stability of the microstructure during the thermal cycles of welding. Hardness profiles typically reveal a hardness peak at the weld centre due to the formation of rapid solidification microstructures, as well as a hardness reduction within the heat-affected zone (HAZ), where dissolution or averaging occurs. For instance, in the Al-Mg-Si series, the dissolution of Mg_2Si precipitates in the HAZ creates a distinct soft zone, which frequently determines the location of tensile failure, resulting in reduced HAZ hardness and strength. Similarly, in Al–Zn–Mg series alloys, extensive averaging of $MgZn_2$ (η) precipitates during welding results in significant softening and lower joint efficiency compared to the base metal. In contrast, Al-Mg series alloys, which are strengthened primarily by solid solution Mg, exhibit more stable HAZ hardness due to limited precipitate dissolution. This contributes to relatively higher joint strength retention [6]. Alloys in the Al-Cu series often experience the greatest strength loss due to the extensive dissolution of Al_2Cu strengthening precipitates, as well as increased susceptibility to hot cracking. This results in poorer mechanical performance of welded joints [55, 56, 57, 58, 59, 60, 61, 62, 63, 64, 65, 66, and 67].

3.5. Fatigue Behavior

The fatigue performance of welded aluminium alloys is significantly impacted by alloy series, microstructural stability in the heat-affected zone (HAZ) and the presence of welding-induced flaws such as porosity and solidification cracks. As fracture initiation tends to occur in the softened HAZ or at the weld toe, where stress concentration is higher, the fatigue strength of laser-welded joints is generally lower than that of the base material [62].

The fatigue resistance of Al-Cu series alloys is greatly reduced after welding due to the widespread dissolution of Al_2Cu strengthening precipitates and the high sensitivity to hot cracking, which creates suitable sites for fatigue crack initiation. Consequently, these alloys exhibit the greatest decrease in fatigue life when fusion-welded among the aluminium series. Due to their solid solution strengthening mechanism and relatively stable microstructure during welding, alloys in the Al-Mg series perform relatively well under fatigue conditions. The lack of considerable precipitate dissolving produces a more consistent hardness profile throughout the joint, delaying the onset of fatigue cracks and raising fatigue endurance limits.

The soft zone that forms in the heat-affected zone (HAZ) due to Mg_2Si precipitate dissolution primarily controls fatigue behaviour in Al-Mg-Si alloys. Compared to the base metal, this localised loss of strength and hardness encourages strain localisation under cyclic loading and fatigue cracks often originate in this area, resulting in a shorter fatigue life [67].

Due to their high static strength, Al-Zn-Mg series alloys demonstrate excellent fatigue resistance in the base material. However, welding results in the severe dissolution of $MgZn_2$ precipitates in the heat-affected zone (HAZ), causing substantial softening and increasing susceptibility to fatigue crack initiation. Furthermore, the fatigue performance of welded joints is compromised by their tendency to crack during solidification and to degrade due to stress corrosion. Figure 3 shows the S-N curves for different types of aluminium alloys. Overall, the fatigue resistance of fusion-welded aluminium alloys generally follows the trend shown below, depending on welding settings, joint shape, and post-weld heat treatment: Al-Mg > Al-Mg-Si ≈ Al-Zn-Mg > Al-Cu [50, 51, 52, 53, 54, 55, 56, 57, 58, 59, 60, 61, 62, 63, 64, 65, 66, and 67].

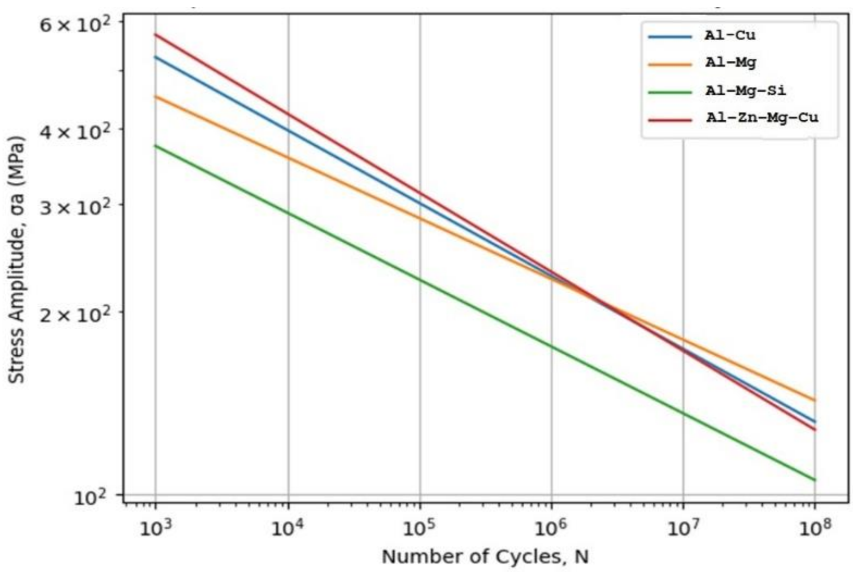

Figure 3. Representative S-N curves for aluminum alloys from different series

4. CONCLUSIONS AND RECOMMENDATIONS

The following conclusions and recommendations regarding the laser welding of aluminium alloys have been established based on the comprehensive analysis of the literature data presented in Tables 1, 2, and 3:

4.1. Conclusions

- **Process versatility and superiority:** Laser beam welding (LBW) has evolved into a highly versatile manufacturing method with applications ranging from the aerospace and automotive industries to joining ultra-thin components. Compared to traditional methods such as TIG welding, which often result in wide heat-affected zones (HAZs) and cracking in the Al-Zn-Mg series of alloys, LBW offers high energy density, a narrow HAZ, and greater flexibility for complex geometries.
- **Material interaction and defect mechanisms:** Although LBW is highly efficient, the interaction between the laser beam and aluminium is more complex than with steels. Key defects such as porosity, solidification cracking, and poor seam geometry remain prevalent. Porosity, in particular, poses a significant challenge: as porosity increases (up to 8.9%, for example), fatigue strength can drop by almost 50% [26], with fractures typically starting near these pores.

- **Microstructural Evolution:** In heat-treatable alloys such as Al-Mg-Si and Al-Zn-Mg, high heat input causes the dissolution of strengthening precipitates. This leads to significant softening in the fusion zone (FZ) and heat-affected zone (HAZ) [43, 45, and 46].
    - In non-heat-treatable alloys (Al-Mg), the evaporation of volatile elements such as magnesium (Mg) affects both keyhole stability and the final chemical composition [23 and 30].
    - CO_2 laser welding specifically contributes to fine-grained structures in the weld metal, enhancing joint strength and influencing fatigue behaviour.
- **Advancements in hybrid systems:** Hybrid laser-MIG welding (LAHW) is superior to autogenous laser welding because it improves gap bridgeability and penetration depth (up to 15 mm), while optimising cooling rates to refine grain growth [27, 34, and 44].
- **Predictive modelling:** The transition from experimental trials to analytical and numerical models has significantly improved the predictability of the process. Numerical simulations have revealed that environmental factors such as CO_2 levels can directly impact peak temperatures and thermal cycles [36].

4.2. Recommendations

- **Defect mitigation strategies:** To eliminate common defects, industrial applications should standardise the use of appropriate filler materials, optimised intermediate shielding gases (such as helium or argon mixtures), and adaptive control systems.
- **Synergistic parameter optimisation:** Future research should focus on the synergistic relationship between defocusing distance, laser power, and shielding gas dynamics, to stabilise the keyhole and minimise technical porosity.
- **Metallurgical restoration:** For high-strength applications involving Al-Mg-Si series alloys, post-weld heat treatment (PWHT) or ageing processes are recommended to restore mechanical integrity lost due to microstructural softening.
- Innovative beam manipulation techniques should be explored to manipulate the beam in ways that were previously impossible. Advanced techniques such as 'rotating laser' or 'oscillating beam' should be further explored to refine grain structures and reduce susceptibility to hot cracking, particularly in the joining of dissimilar metals [44].
- **Advanced simulation integration:** Future experimental work should be integrated with finite element analysis (FEA) and molecular dynamics simulations to improve our understanding of stress concentrations and uniaxial loading behaviours in the fusion zone [31].

CONFLICT OF INTEREST

The author(s) declare that they have no potential conflict of interest.

RESPONSIBILITY

The author of this article declares that they accept responsibility for all ethical, legal, plagiarism, etc. issues that may arise or occur in this study.

FINANCIAL DISCLOSURE

This research received no financial support.

DECLARATION OF ETHICAL STANDARDS

The authors of the article declare that the materials and methods used did not require ethics committee approval and/or regulatory approval.

REFERENCES

[1] Canaby, J.L., et al., (1991). Effects of high temperature surface reaction of aluminum-lithium alloy on the porosity of welded areas. Materials Science and Engineering.
[2] Williams, J.C., et al., (2003). Progress in structural materials for aerospace systems. Acta Materialia.
[3] Gupta, R.K., et al., (2006). Development and characterization of Al-Li alloys. Materials Science and Engineering.
[4] Anyalebechi, P.N., (1995). Analysis of the effects of alloying elements on hydrogen solubility in liquid aluminum alloys. Scripta Metallurgica et Materialia.
[5] Ghaini, F.M., et al., (2009). The relation between liquation and solidification cracks in pulsed laser welding of 2024 aluminium alloy. Materials Science and Engineering.
[6] Shi, Y.W., et al., (2007). Effect of laser beam welding on tear toughness of a 1420 aluminum alloy thin sheet. Materials Science and Engineering.
[7] Lin, D.C.. et al., (2003). A mechanism for the formation of equiaxed grains in welds of aluminum-lithium alloy 2090. Materials Science and Engineering.
[8] Whitaker, I.R., et al. (1994). Fracture of bead-on-plate CO_2 laser welding in the Al-Li alloy 8090. Scripta Metallurgica et Materialia.
[9] Vollertsen, F., et al. (2004). Innovative welding strategies for the manufacture of large aircraft. Welding in the World.
[10] Rengdigs, K.H., (1997). Aluminium structures used in aerospace—status and prospects. Materials Science Forum.
[11] Xiao, R. and Zhang, X., (2014). Problems and issues in laser beam welding of aluminum-lithium alloys. Journal of Manufacturing Processes, 16(2):166-175.
[12] Betoplaser, (n.d.). Laser welding applications for aluminum alloys. Available online.
[13] Karaaslan, A., Yumurtacı, S., and Sönmez, N., (2001). Hardness variations in weld seams of dissimilar materials joined by laser beam welding. II. Makine Malzemesi ve İmalat Teknolojisi Sempozyumu, Manisa.
[14] Beersiek, J., (1999). On-line monitoring of keyhole instabilities during laser beam welding. Prometec GmbH, Aachen.
[15] Çelen, S., Karadeniz, S., and Özden, H., (2008). Effect of laser welding parameters on fusion zone morphological, mechanical and microstructural characteristics of AISI 304 stainless steel. Materialwissenschaft und Werkstofftechnik.
[16] Duley, W.W., Mao, Y.L. and Kinsman, G., (1991). Laser and electron beam welding. Proceedings Conference, Columbia University, New York, USA.
[17] Kahraman, N. and Gülenç, B., (2020). Modern Kaynak Teknolojisi (4th ed.). Ankara: Epa-Mat Basım Yayın Ltd. Şti.
[18] Kovacs, T., (2018). Laser welding process specification base on welding theories. Procedia Manufacturing. 22, 147-153.
[19] Pakdil, M., Çam, G., and Erim, S., (2005). Advantages of laser welding. Makinatek, 95:116-119.
[20] Yavuz, H. and Çam, G., (2005). Laser-arc hybrid welding method. Mühendis ve Makina, 46(543):14-19.

[21] Püskülcü, G. and Koçlular, F., (2009). Laser welding method and applications. Mühendis ve Makina, 50(599):8–17.
[22] Tokdemir, M., Ünlü, B.S., Yılmaz, S.S. and Meriç, C., (2010). Laser welding and its applications. Makinatek, 152:122–128.
[23] Kutsuna, M. and Yan, Q., (1999) Study on porosity formation in laser welds of aluminium alloys (Report 2). Mechanism of porosity formation by hydrogen and magnetism, Welding International, 13:8, 597-611
[24] Vyskoč, M., Sahul, M., Dománková, M., Jurči, P., Sahul, M., Vyskočová, M., and Martinkovič, M., (2020). The Effect of Process Parameters on the Microstructure and Mechanical Properties of AW5083 Aluminum Laser Weld Joints. Metals, 10(11), 1443. https://doi.org/10.3390/met10111443
[25] Atabaki, M.M., Yazdian, N., and Kovacevic, R., (2016). Partial penetration laser-based welding of aluminum alloy (AA 5083-H32). Optik, 127(16), 6782–6804. https://doi.org/10.1016/j.ijleo.2016.05.007
[26] Han, X., Yang, Z., Ma, Y., Shi, C., and Xin, Z., (2020). Porosity distribution and mechanical response of laser-MIG hybrid butt welded 6082-T6 aluminum alloy joint. Optics & Laser Technology, 132, 106511. https://doi.org/10.1016/j.optlastec.2020.106511
[27] Wang, X., Li, B., Li, M., Huang, C., and Chen, H., (2017). Study of local-zone microstructure, strength and fracture toughness of hybrid laser-metal-inert-gas-welded A7N01 aluminum alloy joint. Materials Science and Engineering: A, 688, 114–122. https://doi.org/10.1016/j.msea.2017.01.087
[28] Yan, S., Qin, Q. H., Chen, H., and Zhong, Z., (2020). Hybrid laser welding of dissimilar aluminum alloys: welding processing, microstructure, properties and modelling. Journal of Manufacturing Processes, 56, 295–305. https://doi.org/10.1016/j.jmapro.2020.03.048
[29] Zhao, Y., Zhan, X., Gao, Q., Chen, S., and Kang, Y., (2019). Research on the Microstructure Characteristic and Tensile Property of Laser-MIG Hybrid Welded Joint for 5A06 Aluminum Alloy. Metals and Materials International, 26(3), 346–359. https://doi.org/10.1007/s12540-019-00340-0
[30] Huang, L., Wu, D., Hua, X., Liu, S., Jiang, Z., Li, F., Wang, H., and Shi, S., (2018). Effect of the welding direction on the microstructural characterization in fiber laser-GMAW hybrid welding of 5083 aluminum alloy. Journal of Manufacturing Processes, 31, 514–522. https://doi.org/10.1016/j.jmapro.2017.12.010
[31] Yan, S., Ma, C., and Chen, H., (2020). Modifying microstructures and mechanical properties of laser-arc welded joints of dissimilar advanced aluminum alloys. Materials Characterization, 164, 110331. https://doi.org/10.1016/j.matchar.2020.110331
[32] Nascente, P.A.P., Bolfarini, C., Benassi, C.L., Alcântara, N.G., and Santos, J.F., (2002). Surface and microstructural characterization of laser beam welds in an aluminum alloy. Journal of Vacuum Science & Technology A: Vacuum, Surfaces, and Films, 20(4), 1416–1419. https://doi.org/10.1116/1.1487868
[33] Kang, S. and Shin, J., (2021). The effect of laser beam intensity distribution on weld characteristics in laser welded aluminum alloy (AA5052). Optics & Laser Technology, 142, 107239. https://doi.org/10.1016/j.optlastec.2021.107239
[34] Liu, T., Yan, F., Liu, S., Li, R., Wang, C., and Hu, X., (2016). Microstructure and mechanical properties of laser-arc hybrid

welding joint of GH909 alloy. Optics & Laser Technology, 80, 56–66. https://doi.org/10.1016/j.optlastec.2015.12.020
[35] Katayama, S., Yamaguchi, Y., Mizutani, M., and Matsunawa, A., (1997). Evaluation of mechanical properties of laser-welded aluminum alloy. International Congress on Applications of Lasers & Electro-Optics, G93–G102. https://doi.org/10.2351/1.5059742
[36] Xia, H., Tan, C., Tian, R., Meng, S., Li, L., & Ma, N. (2020). Influence of shielding gas on microstructure and mechanical properties of laser welded-brazed Al/steel lapped joint. Journal of Manufacturing Processes, 54, 347–358. https://doi.org/10.1016/j.jmapro.2020.03.030
[37] Kang, Y., Zhan, X., and Liu, T., (2019). Effect of welding parameters on porosity distribution of dual laser beam bilateral synchronous welding in 2219 aluminum alloy T-joint. Journal of Adhesion Science and Technology, 33(23), 2595–2614. https://doi.org/10.1080/01694243.2019.1650991
[38] Xu, K. and Zhang, S.Q., (2018). Microstructure Analysis of Laser Bonding Welding on Steel-Aluminum. Materials Science Forum, 911, 28–33. https://doi.org/10.4028/www.scientific.net/msf.911.28
[39] Haboudou, A., Peyre, P., Vannes, A. B., and Peix, G., (2003). Reduction of porosity content generated during Nd:YAG laser welding of A356 and AA5083 aluminum alloys. Materials Science and Engineering: A, 363(1–2), 40–52. https://doi.org/10.1016/s0921-5093(03)00637-3
[40] Dai, W., Yang, T., Zhou, Z., Huang, Z., and Chen, H., (2019). Effect of helium-argon shielding gas in laser-metal inert-gas hybrid welded-brazed Al/steel dissimilar joint. Journal of Laser Applications, 31(4). https://doi.org/10.2351/1.5090168
[41] Li, M., Li, Z., Zhao, Y., Li, H., Wang, Y., and Huang, J., (2011). Influence of Welding Parameters on Weld Formation and Microstructure of Dual-Laser Beams Welded T-Joint of Aluminum Alloy. Advances in Materials Science and Engineering, 2011, 1–6. https://doi.org/10.1155/2011/767260
[42] Kuo, T.-Y. and Lin, Y.-T. (2006). Effects of Shielding Gas Flow Rate and Power Waveform on Nd:YAG Laser Welding of A5754-O Aluminum Alloy. Materials Transactions, 47(5), 1365–1373. https://doi.org/10.2320/matertrans.47.1365
[43] El-Batahgy, A. and Kutsuna, M., (2009). Laser Beam Welding of AA5052, AA5083, and AA6061 Aluminum Alloys. Advances in Materials Science and Engineering, 2009(1). Portico. https://doi.org/10.1155/2009/974182
[44] Yang, X., Chen, H., Zhang, C., Zhu, Z., Cai, C., and Huang, S., (2019). Microstructure and stress distribution of narrow-gap rotating laser welding thick Al-Mg alloy joint. Journal of Laser Applications, 31(2). https://doi.org/10.2351/1.5044704
[45] Faye, A., Balcaen, Y., Lacroix, L., and Alexis, J., (2021). Effects of welding parameters on the microstructure and mechanical properties of the AA6061 aluminium alloy joined by a Yb: YAG laser beam. Journal of Advanced Joining Processes, 3, 100047. https://doi.org/10.1016/j.jajp.2021.100047
[46] Chu, Q., Bai, R., Jian, H., Lei, Z., Hu, N., and Yan, C., (2018). Microstructure, texture and mechanical properties of 6061 aluminum laser beam welded joints. Materials Characterization, 137, 269–276. https://doi.org/10.1016/j.matchar.2018.01.030
[47] Braun, R., (2005). Laser beam welding of Al–Mg–Si–Cu alloy 6013 sheet using silicon rich aluminium filler powders. Materials Science and Technology, 21(1), 133–140. https://doi.org/10.1179/174328405x16225

[48] Quan, Y., Chen, Z., Yu, Z., Gong, X., and Li, M., (2008). Characteristics of laser welded wrought Mg-Al-Mn alloy. Materials Characterization, 59(12), 1799-1804. https://doi.org/10.1016/j.matchar.2008.05.001

[49] Oladimeji, O.O. and Taban, E., (2016). Trend and innovations in laser beam welding of wrought aluminum alloys. Welding in the World, 60(3), 415-457. https://doi.org/10.1007/s40194-016-0317-9

[50] Cai, C., Peng, G.C., Li, L. Q., Chen, Y.B., and Qiao, L., (2014). Comparative study on laser welding characteristics of aluminum alloy under atmospheric and sub atmospheric pressures. Science and Technology of Welding and Joining, 19(7), 547-553. https://doi.org/10.1179/1362171814y.0000000223

[51] Mustafa, U., Chandra, M., and Paulraj, S. (2018). Influence of Filler Wire Diameter on Mechanical and Corrosion Properties of AA5083-H111 Al-Mg Alloy Sheets Welded Using an AC Square Wave GTAW Process. *Trans Indian Inst Met* **71**, 1975-1983 (2018). https://doi.org/10.1007/s12666-018-1331-y

[52] Sheikhi, M., Malek Ghaini, F., Torkamany, M. J., & Sabbaghzadeh, J., (2009). Characterisation of solidification cracking in pulsed Nd:YAG laser welding of 2024 aluminium alloy. Science and Technology of Welding and Joining, 14(2), 161-165. https://doi.org/10.1179/136217108x386554

[53] Kou, S., (2003) *Welding Metallurgy*, 2nd edition, John Wiley, New York.

[54] Davis J.R., (1993). Aluminum and Aluminum Alloys, in ASM Specially Handbook, ASM International, Metal Park, Ohio

[55] Joseph R., (1993). Davis, ''Aluminum and Aluminum Alloys'', ASM İnternational

[56] Sayılgan, S., (2009). Production and Characterization of High Performance AlFe-Si-V Alloys for Elevated Temperature Applications, Yüksek Lisans Tezi, O.D.T.Ü Fen Bilimleri Enstitüsü, Ankara, Türkiye.

[57] Spear, K.E., Visco S., Wuchina E.J., and Wachsman E.D., (2006). High temperature materials, The Electrochemical Society Interface, 48-51.

[58] Darıdereli, Y., (2010). Alüminyum Alaşımlarının Mikroyapı, Mekanik Özellikleri ve Aşınma Direncine Yaşlanmanın Etkisi'', İÜ FBE Yüksek Lisans Tezi.

[59] Aykut, D., (2018). Ekrem Altuncu, Yüksek Sıcaklığa Dirençli Alüminyum Alaşımı Pistonlar, Tarih : 2018-05-28,Metal dünyası yayınları.

[60] Li, Y., Yang, B., Zhang, M., Wang, H., Gong, W., Lai, R., Li, Y., and Teng, J., (2023). The corrosion behavior and mechanical properties of 5083 Al-Mg alloy manufactured by additive friction stir deposition. Corrosion Science, 213, 110972. https://doi.org/10.1016/j.corsci.2023.110972.

[61] Ma, G., Zhang, C., and Liu, Y., (2024). Investigation of laser welding characteristics under varied oscillation patterns. Optics & Laser Technology, 169, 110059. https://doi.org/10.1016/j.optlastec.2023.110059

[62] Dong, W., Li, H., and Chen, J., (2025). Effect of welding parameters on joint quality and microstructure in aluminum alloys, Journal of Manufacturing Processes 151 (2025) 426-433. https://doi.org/10.1016/j.jmapro.2025.07.050

[63] Huang, S., Zhou, M., and Wang, Q., (2024). Microstructural evolution and mechanical properties of welded aluminum alloys. Journal of Manufacturing Processes, 113, 307-318. https://doi.org/10.1016/j.jmapro.2024.01.060

[64] Wang, L., Smith, J., and Johnson, R., (2016). Effect of beam oscillation pattern on weld characterization of laser welding of AA6061-T6 aluminum alloy. Materials & Design, 108, 707–717. https://doi.org/10.1016/j.matdes.2016.07.053
[65] Hu, K., Li, X., and Chen, Z., (2022). Microstructure and performance of welded Al-Mg-Si series aluminum alloys. Materials Science and Engineering: A, 832, 142431. https://doi.org/10.1016/j.msea.2021.142431
[66] Wang, L., Xu, T., and Zhao, Y., (2025). Advanced processing techniques for aluminum alloy welds. Journal of Materials Processing Technology, 118883. https://doi.org/10.1016/j.jmatprotec.2025.118883
[67] Yang, H., Ji, X., Cheng, R., Liu, C., Wang, X., Niu, F., and Guo, Y., (2026). Improving weld quality of 6061/7075 dissimilar aluminum alloy joints using laser oscillation welding. Materials Letters, 405, 139743. https://doi.org/10.1016/j.matlet.2025.139743